available online at www.sciencedirect.com

ScienceDirect

Geochimica et Cosmochimica Acta 123 (2013) 17–34

Geochimica et Cosmochimica Acta

www.elsevier.com/locate/gca

The Genesis solar xenon composition and its relationship to planetary xenon signatures

S.A. Crowther *, J.D. Gilmour

School of Earth, Atmospheric and Environmental Sciences, The University of Manchester, Oxford Road, Manchester M13 9PL, UK

Received 15 March 2013; accepted in revised form 6 September 2013; available online 17 September 2013

Abstract

The fluence and isotopic composition of solar wind xenon have been determined from silicon collector targets flown on the NASA Genesis mission. A protocol was developed to extract gas quantitatively from samples of ~9–25 mm^2, and xenon measured using the RELAX mass spectrometer. The fluence of implanted solar wind xenon is 1.202(87) × 10^6 atoms ^{132}Xe cm^{-2}, which equates to a flux of 5.14(21) × 10^6 atoms ^{132}Xe cm^{-2} year^{-1} at the L1 point. This value is in good agreement with those reported in other studies. The isotopic composition of the solar wind is consistent with that extracted from the young lunar regolith and other Genesis collector targets.

The more precise xenon isotopic data derived from the Genesis mission confirm models of relationships among planetary xenon signatures. The underlying composition of Xe-Q is mass fractionated solar wind; small, varying contributions of Xe-HL and ^{129}Xe from ^{129}I decay are present in reported meteorite analyses. In contrast, an s-process deficit is apparent in Xe-P3, which appears to have been mass fractionated to the same extent as Xe-Q from a precursor composition, suggesting similar trapping mechanisms. Solar wind xenon later evolved by the addition of ~1% (at ^{132}Xe) of s-process xenon to this precursor. As an alternative model to a single source reservoir for Xe-P3, we propose that trapping of xenon onto carbonaceous carriers has been an ongoing process across galactic history, and that preparation of the residues in which Xe-P3 has been identified preferentially preserves longer lived host phases; a higher proportion of these sample xenon isotopic compositions from earlier in galactic chemical evolution, allowing the s-process deficit to become apparent. The relationships among SW-Xe, Xe-Q and Xe-P3 predict that the ^{124}Xe/^{132}Xe ratio for the solar wind is 0.00481(6).

1. INTRODUCTION

The solar system is believed to have formed from a molecular cloud which collapsed to form an early star and an accretion disk known as the solar nebula (e.g. Russell, 2007). The planets and other solar system bodies formed in this disk. The formation processes of solar system bodies left traces in their elemental and isotopic compositions, but to fully interpret them it is necessary to know the bulk elemental and isotopic composition of the solar nebula from which the bodies formed. This can be achieved by measuring the solar composition. The sun accounts for 99.86% of the mass of the solar system so its initial composition was the average starting composition of a well mixed solar system. With the exceptions of deuterium and lithium, the mean elemental and isotopic compositions of the solar photosphere, as sampled by the solar wind, are believed to represent this initial composition with only minor differences due to fractionation (Turcotte and Wimmer-Schweingruber, 2002; Wiens et al., 2004). The Genesis mission sampled the present day solar wind, with the aim of determining elemental and isotopic

* Corresponding author. Tel.: +44 0 161 275 0407.
E-mail address: sarah.crowther@manchester.ac.uk (S.A. Crowther).

0016-7037
http://dx.doi.org/10.1016/j.gca.2013.09.007

compositions with sufficient precision to improve our understanding of the formation and evolution of the solar system (Burnett et al., 2003).

The traces of formation and evolutionary processes left in noble gas isotopic compositions are key to understanding the volatile evolution of solar system reservoirs, so determining their solar compositions is particularly important; measuring the elemental and isotopic composition of the noble gases (especially the heavy noble gases) is one of the highest priority scientific objectives of the Genesis mission (Burnett et al., 2003). It is also particularly difficult. Noble gas absorption lines are not observed in spectra of the solar photosphere. The solar compositions of the lighter noble gases were determined from the Apollo Solar Wind Composition (SWC) experiments (Geiss et al., 2004), in which aluminium foils were exposed to the solar wind on the lunar surface for periods of up to 45 h. However the concentrations of krypton and xenon in these foils were below detection limits. Before the Genesis mission, the most accurate solar wind data for neon and argon, and the only available solar wind compositions of krypton and xenon, resulted from measurement of material from extraterrestrial regoliths, especially the young lunar regolith (YLR), i.e. samples irradiated by the solar wind on the surface of the Moon within the last ~100 Ma (Benkert et al., 1993; Wieler and Baur, 1994; Pepin et al., 1995; Palma et al., 2002). However noble gas data from the lunar regolith is potentially affected by other components such as fission and spallation products, the relative contributions of which are difficult to correct for because of uncertainties in their isotopic compositions and the varying chemistry of the material. This leads to some uncertainty in the solar wind isotopic compositions obtained in this manner. The long exposure times of Genesis collectors provide an opportunity to make measurements of directly sampled solar wind without the added complications of spallation or fission components in the lunar regolith samples. Contributions from other components can be corrected for or constrained by analysis of identical unflown samples of the collector materials.

In this work we focus on xenon. The accepted isotopic compositions of both Xe-Q, the major xenon component trapped in meteorites (Busemann et al., 2000), and terrestrial atmospheric xenon (Basford et al., 1973) cannot be derived directly from the solar wind xenon composition (as measured in the YLR) (Pepin et al., 1995) by linear mass fractionation alone. Nor can a third similar component that is observed in nanodiamond-rich residues (Xe-P3) (Huss and Lewis, 1994). Gilmour (2010) showed that Xe-Q can be understood as mass fractionated solar xenon (as measured in the YLR) with the addition of variable amounts of excess ^{129}Xe from decay of ^{129}I and of Xe-HL, a presolar component enriched in heavy isotopes that is associated with nanodiamonds isolated from primitive meteorites (Huss and Lewis, 1994). A second meteoritic component, labelled Xe-P3, is also of interest. It is released from nanodiamond residues during low temperature heating. Although it is a similar mix of contributions from various nucleosynthetic sources as Xe-Q, and is fractionated to around the same extent, it is slightly deficient in s-process isotopes compared to mass fractionated solar xenon (Gilmour, 2010). Atmospheric xenon shows an excess of ^{129}Xe and is depleted in ^{134,136}Xe relative to mass fractionated solar xenon. The ^{129}Xe excess is again believed to be the product of ^{129}I decay. The ^{134,136}Xe depletions, however, are much more difficult to explain. The observed ratios cannot be obtained from *addition* of spontaneous fission products from ^{244}Pu and ^{238}U to mass fractionated solar wind. It has been proposed that the Earth's atmosphere sampled a xenon reservoir distinct from the well mixed solar system, which was depleted in the heavier isotopes relative to mass fractionated solar xenon (Pepin, 2000). This proposed component is labelled U-Xe, but to date there is no separate experimental evidence for it.

Here we report the abundance and isotopic composition of xenon released from Genesis mission silicon collectors, compare it to the results of other workers, and consider whether the proposed relationships among bulk solar system xenon reservoirs outlined above survive the improved precision in the solar xenon composition derived from Genesis mission data.

2. THE GENESIS MISSION

NASA's Genesis mission (Burnett et al., 2003) was launched in August 2001. The spacecraft spent about two and a half years collecting solar wind in a halo orbit around the L1 Lagrangian point. Samples were returned to Earth for elemental and isotopic analyses in September 2004. Solar wind ions were implanted into collector arrays composed of hexagonal wafers of nine different types of ultra-pure material (Jurewicz et al., 2003). Two bulk collector arrays were continuously exposed to the solar wind for a total of 852.83 days (Reisenfeld et al., 2007). These arrays have the longest solar wind exposure time to date of any artificial material, more than 400 times longer than any of the SWC foils exposed during the Apollo programme (Geiss et al., 2004). The concentrations of implanted solar wind are consequently much higher than in the SWC foils.

3. PREVIOUS WORK

We reported the first isotopic analysis of solar wind xenon sampled by the Genesis mission in 2008 (Crowther et al., 2008a; Burnett et al., 2011), and have previously published details of refinements in our analytical technique and a preliminary composition for directly collected solar wind (Crowther and Gilmour, 2012). In our initial experiments xenon was extracted from silicon collector targets by infra red laser heating, but ultra violet laser ablation proved to be a superior extraction method. We showed that, for the major isotopes $^{129-136}$Xe, the xenon isotopic composition of solar wind sampled by the Genesis mission is consistent with that determined from samples of the YLR (Pepin et al., 1995), with at most minor (<5‰ per amu) mass fractionation favouring the heavier isotopes. We determined a preliminary value of 1.0474(75) for the ^{129}Xe/^{132}Xe ratio, which is in excellent agreement with the value of 1.042(9) measured in the YLR (Pepin et al., 1995). With the

exception of the $^{131}Xe/^{132}Xe$ ratio, all the preliminary ratios are within uncertainty of the lunar values.

Heber et al. (2009) and Vogel et al. (2011) have measured the solar wind ^{132}Xe concentration and $^{129}Xe/^{132}Xe$ ratio in silicon collector targets from the bulk collector arrays. UV laser ablation was used to extract the implanted solar wind from samples with areas typically between about 4 and 60 mm^2. ^{129}Xe and ^{132}Xe were measured in conjunction with $^{36,38,40}Ar$ and $^{84,86}Kr$. Vogel et al. (2011) determined the ^{132}Xe concentration to be $1.25(9) \times 10^6$ atoms $^{132}Xe\ cm^{-2}$ and the $^{129}Xe/^{132}Xe$ ratios as 1.06(1) from the mean and standard error of 12 analyses. This $^{129}Xe/^{132}Xe$ ratio is within uncertainty of the ratio measured in the YLR (Pepin et al., 1995) and our preliminary ratio (Crowther and Gilmour, 2012). The measured concentration is somewhat higher than the pre-flight estimate of $\sim 3 \times 10^6$ atoms total Xe cm^{-2}, or $\sim 8 \times 10^5$ atoms $^{132}Xe\ cm^{-2}$ (Burnett et al., 2003).

Meshik et al. (2012) have reported compositional data for all isotopes of both xenon and krypton in the polished aluminium (PAC) and aluminium-on-sapphire (AloS) collector targets from the bulk collector arrays. Laser ablation was used to extract the solar wind from the collector targets, using an IR laser (1064 nm) for the AloS targets and a UV laser (266 nm) for the PAC. Xenon and krypton were measured simultaneously, and the $^{84}Kr/^{132}Xe$ ratio assumed to be a binary mixture of solar wind and a trapped, terrestrial component. They determined the xenon fluence to be $1.15(4) \times 10^6$ atoms $^{132}Xe\ cm^{-2}$, which again is slightly higher than the pre-flight estimate (Burnett et al., 2003), but agrees (within uncertainty) with the concentration determined by Vogel et al. (2011). Their $^{129}Xe/^{132}Xe$ ratio is 1.0401(10), which is somewhat lower than the ratio measured by Vogel et al. (2011), but in excellent agreement with both the ratio measured in the YLR (Pepin et al., 1995) and our preliminary Genesis ratio (Crowther and Gilmour, 2012). All the ratios are within uncertainty of the lunar values.

4. EXPERIMENTAL TECHNIQUES

We use RELAX (Refrigerator Enhanced Laser Analyser for Xenon) (Gilmour et al., 1991, 1994; Crowther et al., 2008b) to measure the concentration and isotopic composition of xenon in the present-day solar wind sampled by the Genesis mission. RELAX is a resonance ionization, time-of-flight mass spectrometer, specifically designed to measure xenon isotope ratios in extraterrestrial samples. RELAX can determine xenon isotope ratios from just a few thousand atoms of xenon, although precision naturally increases with sample size. Samples are limited to about 10^6 atoms, but precision can be improved by averaging analyses when multiple aliquots are available. We have previously demonstrated the reproducibility of RELAX measurements, and that the ratios of the major isotopes can be determined to within 1.5‰ in this manner (Crowther et al., 2008b). We have applied this technique of analysing multiple small samples to this work.

In the analyses reported here, samples were loaded into the laser extraction port and baked overnight for 12 h to a peak temperature of 150 °C using a combination of heating tapes (around the extraction lines) and a heat lamp (directed onto the laser port), following our usual protocol. This typically results in procedural blanks below 1000 atoms ^{132}Xe – mean blanks for 3 separate sets of analyses performed during this work are given in Table 1. Gas extracted from the collector material (both flight and non-flight samples) was gettered (SAES, sintered Zr, ~350 °C) for one minute to remove active gasses before being admitted into the mass spectrometer.

Xenon in the mass spectrometer continuously condenses on a localised cold spot (80 K) in the ion source. Pulses from an infra red heating laser ($\lambda = 1064$ nm, 5 mJ 10 ns pulse) release gas from this cold spot every 0.1 s. The ionising laser ($\lambda = 249.6$ nm, 2 mJ) is fired through the resulting plume when the concentration in the ionising region reaches a maximum, selectively ionising xenon. The xenon ions are separated according to their mass by the time of flight mass spectrometer, and microchannel plate detectors (MCPs) allow the detection of all xenon isotopes from each laser pulse.

In this work analyses follow the protocol described by Crowther et al. (2008b). Data from 3000 consecutive cycles are acquired over a 5 min period. These are summed over 10 s intervals, to produce 30 single mass spectra which correspond to the integrated signal detected for each isotope in that interval. The peak height of a normalising isotope and the ratios of the other isotopes normalised to this isotope are determined for each of the 30 individual spectra. Trends in these quantities are extrapolated to determine their values at the time gas was admitted into the mass spectrometer. Air calibrations and procedural blanks are interspersed between sample analyses. Air calibrations allow the absolute quantities of gas to be calculated and a correction to be made for instrument mass discrimination. The quantity of ^{132}Xe in the samples is calculated by comparing peak heights with those of the air calibrations that contain a known amount of gas. The peak heights of the air calibrations show some variations (standard deviation of the mean ranged between about 11% and 17% for the 3 sets of analyses carried out in this work) due to variations in instrument sensitivity. All data discussed here have been corrected for procedural blank, which included contributions from both xenon and residual hydrocarbons. Average procedural blanks carried out during these analyses are given in Table 1.

4.1. Samples

Czochralski-grown silicon (CZ-Si) wafers (Jurewicz et al., 2003) from the bulk collector array have been used in this work. Samples flown on board the spacecraft and exposed to the solar wind ("flight samples") contain both implanted solar wind xenon and blank xenon intrinsic to the wafer material or the extraction process. The composition and concentration of the intrinsic xenon is assessed by analysing pieces of identical wafers that were not flown on board the spacecraft ("non-flight samples") in conjunction with analyses of the flight samples.

Instrumental mass fractionation can best be corrected for when sample sizes are closely matched to those of calibration aliquots of known composition. Aliquots from the

Table 1
Mean procedural blanks measured for 3 separate sets of analyses performed during this work. Isobaric hydrocarbons interfere (in particular) with the ^{126}Xe and ^{128}Xe peaks, leading to measured compositions which are difference from atmospheric xenon.

Analyses Set	No. blanks averaged	Atoms ^{132}Xe	^{124}Xe/^{132}Xe	^{126}Xe/^{132}Xe	^{128}Xe/^{132}Xe	^{129}Xe/^{132}Xe	^{130}Xe/^{132}Xe	^{131}Xe/^{132}Xe	^{134}Xe/^{132}Xe	^{136}Xe/^{132}Xe
Set 1	69	987 (379)	n.d.	0.084 (68)	3.7 (1.9)	1.04 (18)	0.114 (54)	0.59 (12)	0.26 (13)	0.145 (75)
Set 2	64	743 (314)	n.d.	0.051 (62)	1.6 (1.1)	1.04 (18)	0.093 (53)	0.69 (14)	0.21 (11)	0.193 (90)
Set 3	43	987 (422)	n.d.	0.089 (72)	6.3 (2.8)	1.28 (31)	0.121 (71)	0.57 (17)	0.06 (162)	0.123 (73)

Numbers in parentheses represent 1 standard deviation uncertainties in the unit of the last decimal place quoted.

smaller of two RELAX air calibration samples contain 1.2×10^5 atoms of atmospheric ^{132}Xe (Crowther et al., 2008b). Pre-mission calculations predicted the 2-year fluence for solar wind xenon implanted into the bulk collector arrays to be 3.0×10^6 atoms cm^{-2} (Burnett et al., 2003). Combining this value and the solar wind composition measured in the young lunar regolith (Pepin et al., 1995), the ^{132}Xe concentration was estimated to be $\sim 8 \times 10^5$ atoms ^{132}Xe cm^{-2}. Therefore we chose to analyse approximately square samples with areas typically 9–25 mm^2 (dimensions typically 3–5 mm) such that the expected amount of ^{132}Xe is closely matched to that in the calibration aliquots.

The dimensions and areas of the actual polished collector surface of all samples were measured by the Genesis Solar Wind Sample Curation Team prior to analysis (Table 2). ^{132}Xe concentrations (atoms cm^{-2}) have been calculated from the sample surface areas measured by the Curation Team.

All samples (flight and non-flight) were also cleaned by the Genesis Solar Wind Sample Curation Team prior to analysis. Samples were first cleaned with ultra-pure water (UPW) in a megasonic spinner (5 or 15 min at 40 °C, 3000 rmp) to remove any surface particles (Calaway et al., 2009). This was followed by ultraviolet–ozone (UV/O_3) cleaning (30 min) to remove "brown stain" contamination (Sestak et al., 2006; Calaway et al., 2007).

4.2. Gas extraction

As described in our previous publication, our preferred extraction technique uses a frequency tripled Nd:YAG laser (Continuum 9010, $\lambda = 355$ nm, 350 mJ) to ablate the surfaces of the samples. Investigations showed that multiple low energy density laser shots are more successful at extracting the solar wind and minimising blank contributions than individual high energy density shots (Crowther and Gilmour, 2012). Therefore it was not necessary to focus the beam to a small spot with a high energy density, but instead an unfocused, low energy density beam (nominally 550 mJ cm^{-2}) was used. The ~9 mm beam from this laser has a uniform profile across the central ~6 mm, wide enough to cover and ablate the whole surface of the ~3–5 mm square samples used in this study without the need to raster over the surface.

Preliminary indications were that about 30 laser shots extracted all the implanted solar wind, and the following protocol was initially adopted. Gas released by a single initial laser shot was analysed to separate any surface adsorbed contamination. This was followed by analysis of gas extracted by 30 consecutive laser shots (this was designated *1 + 30*). Data from some such analyses were previously published (Crowther and Gilmour, 2012) for some of the samples discussed here (as indicated in Tables 2 and 3). This was followed by a further 4 analyses of 30 consecutive laser shots to allow the presence of more deeply implanted solar wind to be investigated. Then a final analysis of 150 laser shots was performed to investigate the intrinsic xenon at depth.

In our previous work we reported indications that the ^{132}Xe concentration measured in the later 4 × 30-shot

analyses of the flight samples was higher than those measured in the non-flight samples (Crowther and Gilmour, 2012). However it was difficult to make a definitive statement in light of the significant variations observed in the concentrations of intrinsic xenon in the non-flight samples. The quantities of gas extracted in the individual analyses were too small to determine the isotopic compositions with the precision required to confirm whether those from the flight samples included a contribution from the solar wind. Therefore in subsequent analyses this was replaced with a single 120-shot analysis and the following preferred protocol adopted:

1. Analysis of xenon extracted by a single initial laser shot, to separate any surface adsorbed component,
2. Analysis of 30 consecutive laser shots to extract the majority of the implanted solar wind,
3. Analysis of 120 consecutive laser shots to investigate any more deeply implanted solar wind, and
4. A final analysis of 150 consecutive laser shots to investigate the intrinsic xenon at depth.

The initial, single laser shot analysis was intended to separate surface adsorbed, atmospheric contamination from the implanted solar wind in the flight samples. With the exception of sample 60927, this analysis included a contribution from the solar wind; sample 60927 was the only sample where the gas extracted in this step had an atmospheric isotopic composition. The average flight sample has about 3 times more xenon in this extraction than the average non-flight sample. The blank xenon extracted from the average non-flight samples in this step accounts for ~3% of the total amount of gas extracted from the average flight sample in all extraction steps. The difference between the average gas content of the flight and non-flight samples in this step amounts to ~9% of the total gas excess in the flight samples.

The larger quantities of gas in the 120-shot extraction (compared with any of 4 individual 30-shot extractions in earlier analyses) allowed more precise isotope ratios to be determined for these analyses. The measured isotope ratios in this extraction from the flight samples tended to show enrichments in the lighter isotopes and depletions in the heavier isotopes relative to the atmospheric compositions, suggesting that this extraction did indeed include a small fraction of the solar wind. The average flight sample has about 50% more xenon in this release than the average non-flight sample. The difference between the average gas content of the flight and non-flight samples in this depth interval amounts to ~16% of the total gas excess in the flight samples. However as noted above, the variations in the concentration of intrinsic xenon mean it is difficult to make a definitive statement.

The gas analyses in the final, 150-shot extraction from the flight samples was identical, within uncertainty, to atmospheric xenon. There was no significant difference between the average ^{132}Xe concentration measured in the flight samples for this extraction and that measured in the non-flight samples. Therefore it was assumed that no implanted solar wind contributed to this extraction in the flight samples, and that all the solar wind had been extracted by the previous three analyses. This extraction was not included in the data in Table 3 or when calculating the concentration and composition of the solar wind. It does, however, serve to test whether the concentration of intrinsic xenon at depth can be used to make a correction to the ^{132}Xe concentrations measured in the implantation depth interval.

5. RESULTS AND DISCUSSION

The measured ^{132}Xe concentrations and isotope ratios for 16 flight and 15 non-flight samples are given in Table 3. These data are the sum of the first three extractions described above: a single-shot analysis plus a 30-shot analysis plus a 120-shot analysis. In some cases (as indicated) 4 separate 30-shot extractions were summed in place of a single 120 shot analysis. The initial, single laser shot analysis is not included for sample 60927, as this extraction contained only atmospheric xenon: for this sample only the 30- and 120-shot analyses are summed together.

Blank xenon intrinsic to the collector targets, measured in the non-flight samples, is isotopically identical (within uncertainty) to atmospheric xenon (Table 3). The histogram in Fig. 1 shows that the ^{132}Xe concentrations in the majority of non-flight samples cluster together, with what appear to be four high concentration outliers. The ^{132}Xe concentrations measured in these outliers are significantly different from the concentrations measured in the other samples. The variations are more than would be expected from the variations in the sensitivity (as determined from the air calibrations), suggesting that the concentration of the underlying blank is variable. The evidence suggests that the concentrations of blank xenon do not just adhere to a Normal distribution, but occasional samples contain excess blank xenon. If these outliers are excluded, the ^{132}Xe concentrations in the remaining 11 non-flight samples vary by ~50%, (variation is measured as standard deviation divided by average of the distribution of the included points). If one or more of these are included the ^{132}Xe concentrations vary by >80%.

Flight samples contain a mixture of implanted solar wind xenon and blank intrinsic xenon (as identified in the non-flight samples). Similarly to the non-flight samples, the ^{132}Xe concentrations in the vast majority of samples cluster together, with two high concentration outliers that appear significantly different from the concentrations measured in the other samples given their uncertainties (Table 3, Fig. 1). We would expect percentage variations to be lower in this case, since the contribution from solar wind is expected to be a constant contribution to the average. In this case, inclusion of the lowest concentration of these outliers changes the variation in ^{132}Xe concentration of flight samples from 19%, consistent with the variation in sensitivity as measured by air calibrations (around 11–17%), to 36%.

Another way to examine outliers is to consider how many standard deviations they are away from the average of the distribution of which they form a part. If the lowest concentration outlier is included it is found to lie 2.8 standard deviations above the mean in the case of the

Table 2
Summary of all CZ-Si Genesis samples analysed in this work.

JSC sample No.	Dimensions (mm)[a]	Area (mm^2)[b]	Mass (mg)
Flight samples			
60927[c]	4.20 × 3.30	10.192	15.83
60928[c]	3.87 × 3.43	8.456	15.23
60951[c]	4.64 × 4.35	13.536	22.71
60943[c]	4.40 × 4.04	12.82	21.07
60941[c]	5.97 × 3.75	16.955	26.23
60945[c]	3.60 × 3.55	8.211	12.95
60948[c]	6.76 × 3.77	14.912	25.62
60937	4.67 × 3.51	9.552	17.54
60950	4.77 × 3.87	12.246	21.65
60944	4.60 × 3.29	10.785	19.10
60940	5.06 × 4.01	12.431	23.21
60942	4.81 × 3.90	11.126	21.50
60938	4.51 × 3.89	11.165	20.63
60929	5.59 × 4.81	15.144	29.18
60952	5.46 × 3.48	12.316	22.09
60930	5.91 × 4.63	19.633	35.97
Non-flight samples			
3CZ00327 7,0[c]	5. 70 × 4.78	4.781	31.97
3CZ00327 4,0[c]	5.38 × 4.63	17.321	29.00
3CZ00327 1,0[c]	5.97 × 5.77	24.677	41.30
3CZ00327 9,0[c]	5.53 × 4.06	16.48	26.63
3CZ00327 10,0[c]	5.86 × 5.76	22.103	39.13
3CZ00327 20[c]	4.63 × 3.97	14.822	23.92
3CZ00327 22[c]	5.46 × 5.08	20.544	33.16
3CZ00327 21[c]	4.47 × 3.64	10.737	21.51
3CZ00327 23[c]	5.76 × 4.04	15.351	29.57
3CZ00327 24	4.14 × 3.57	9.114	16.83
3CZ00327 25	6.09 × 4.85	18.009	33.45
3CZ00327 26	4.39 × 3.96	13.559	21.52
3CZ00327 27	4.74 × 4.12	12.564	23.67
3CZ00327 28	4.77 × 4.39	15.942	26.82
3CZ00327 29	4.55 × 3.64	11.295	19.84

[a] Dimensions measured by the Genesis Solar Wind Sample Curation Team. The length refers to the widest part of the longest axis; the width is always measured perpendicular to the length. Most dimensions have been measured to 3 decimal places, but are quoted to 2 decimal places here as there is the potential for some uncertainty in the 3rd decimal place (Burkett, 2013, Pers. comm.).

[b] Actual area of the polished collector surface calculated by the Genesis Solar Wind Sample Curation Team using Canvas 10 software (Burkett et al., 2011). The area is calculated from selected pixels calibrated to a micron scale (Burkett, 2013, Pers. comm.); it is independent from the length and width measurements. Chips adjacent to the edge are excluded from the area calculation; however any chips or scratches not touching the edges are included. Only samples designated as "good", meaning they are relatively free from surface imperfections, were selected for this work. These areas were used to calculate ^{132}Xe concentrations for the individual samples.

[c] Preliminary ^{132}Xe concentrations and isotope ratios for *1 + 30* laser shot analyses for these samples were published in our previous paper (Crowther and Gilmour, 2012).

non-flight samples, and 3.2 standard deviations above the mean in the case of flight samples. The highest concentration points which we do not reject as outliers lie 1.7 and 2.3 standard deviations above the mean of their respective distributions, and might also be considered to be low probability events given the number of analyses. Rejecting one or more of them leads to no more than 4% variation in the derived concentration of solar wind, compared to our quoted 7% 1σ uncertainty.

Assuming the xenon extracted from the flight samples is the sum of a constant concentration implanted solar wind xenon component mixed with variable concentrations of intrinsic xenon, we would expect to observe linear correlations between the measured isotope ratios and the reciprocal of the concentration of the normalising isotope. For instance, the $^{129}Xe/^{132}Xe$ ratio should be related to the ^{132}Xe concentration ($[^{132}Xe]$) by the equation:

$$\left(\frac{^{129}Xe}{^{132}Xe}\right)_M = k\left(\frac{1}{[^{132}Xe]_M}\right) + \left(\frac{^{129}Xe}{^{132}Xe}\right)_{IB} \quad (1)$$

where the subscript *M* denotes measured values, *IB* refers to the intrinsic blank and the square brackets denote concentration. Such correlations are observed, as shown in Fig. 2. The mixing lines indicate that the implanted solar wind component is enriched in the lighter isotopes and depleted in the heavier isotopes relative to the composition of atmospheric xenon. In order to determine the solar wind compositions from the mixing lines shown in Fig. 2, it is

Table 3
Measured ^{132}Xe concentration and isotope ratios for 16 flight and 15 non-flight samples. Except where otherwise indicated, data are the sum of 3 analyses totalling 150 laser shots: a single laser shot initial analysis, followed by analysis of the gas extracted by 30 consecutive laser shots, and then analysis of that from 120 consecutive laser shots.

Sample	Atoms ^{132}Xe per cm^2 ($\times 10^6$)	^{124}Xe/^{132}Xe	^{126}Xe/^{132}Xe	^{128}Xe/^{132}Xe	^{129}Xe/^{132}Xe	^{130}Xe/^{132}Xe	^{131}Xe/^{132}Xe	^{134}Xe/^{136}Xe	^{136}Xe/^{132}Xe
Flight samples									
60927[a, b]	6.066 (173)[c]	0.0041 (5)	0.0032 (6)	0.069 (12)	0.997 (6)	0.163 (2)	0.8066 (5)	0.395 (3)	0.331 (3)
60928[a]	3.517 (98)[c]	0.0040 (10)	0.0004 (12)	0.037 (26)	1.005 (10)	0.165 (3)	0.816 (8)	0.384 (5)	0.325 (4)
60951[a]	1.451 (41)	0.0041 (11)	0.0043 (14)	0.084 (20)	1.024 (12)	0.170 (4)	0.815 (10)	0.379 (6)	0.297 (5)
60943[a]	1.490 (44)	0.0041 (12)	0.0033 (16)	0.075 (20)	1.056 (11)	0.164 (3)	0.823 (9)	0.382 (5)	0.302 (5)
60941[a]	1.268 (26)	0.0042 (11)	0.0040 (14)	0.076 (18)	1.053 (11)	0.169 (3)	0.819 (9)	0.371 (5)	0.303 (4)
60945[a]	1.726 (63)	0.0062 (19)	0.0070 (24)	0.091 (27)	1.022 (13)	0.163 (4)	0.798 (11)	0.368 (6)	0.302 (5)
60948[a]	1.264 (36)	0.0039 (16)	0.0085 (21)	0.117 (21)	1.030 (13)	0.167 (4)	0.807 (10)	0.361 (6)	0.299 (5)
60937	1.695 (80)	0.0041 (15)	0.0004 (19)	0.018 (83)	1.041 (17)	0.161 (5)	0.815 (14)	0.364 (8)	0.301 (7)
60950	1.562 (64)	0.0044 (13)	0.0032 (16)	0.037 (70)	1.037 (15)	0.163 (4)	0.815 (11)	0.372 (7)	0.305 (6)
60944	1.390 (61)	0.0049 (18)	0.0034 (23)	0.124 (92)	1.049 (23)	0.165 (7)	0.833 (18)	0.378 (11)	0.311 (10)
60940	1.114 (40)	0.0046 (18)	0.0016 (23)	n.d.	1.021 (20)	0.160 (6)	0.817 (15)	0.367 (9)	0.306 (8)
60942	1.262 (42)	0.0041 (16)	0.0021 (23)	n.d.	1.033 (20)	0.168 (6)	0.835 (16)	0.384 (9)	0.309 (8)
60938	2.171 (90)	0.0048 (11)	0.0036 (14)	0.069 (56)	1.016 (13)	0.161 (4)	0.817 (10)	0.360 (6)	0.305 (5)
60929	1.819 (105)	0.0056 (11)	0.0045 (14)	0.118 (51)	1.037 (13)	0.166 (4)	0.819 (11)	0.373 (6)	0.303 (6)
60952	1.544 (87)	0.0041 (15)	0.0019 (17)	0.000	1.014 (16)	0.159 (5)	0.812 (13)	0.373 (8)	0.302 (7)
60930	1.253 (62)	n.d.	0.0039 (14)	0.013 (55)	1.035 (13)	0.168 (4)	0.817 (10)	0.372 (6)	0.309 (5)
Mean	1.501 (75)								
Non-flight samples									
3CZ00327 7,0[a]	2.281 (54)[c]	0.0035 (7)	0.0016 (9)	0.020 (20)	0.977 (8)	0.150 (2)	0.787 (7)	0.392 (4)	0.337 (4)
3CZ00327 4,0[a]	0.243 (7)	0.0108 (48)	n.d.	0.052 (90)	1.015 (35)	0.157 (9)	0.802 (28)	0.421 (16)	0.363 (14)
3CZ00327 1,0[a]	0.093 (4)	n.d.	0.0013 (107)	0.050 (165)	0.983 (57)	0.158 (14)	0.824 (46)	0.394 (23)	0.350 (21)
3CZ00327 9,0[a]	0.138 (6)	0.0135 (82)	0.0293 (115)	0.088 (168)	1.011 (58)	n.d.	0.758 (45)	0.391 (23)	0.351 (21)
3CZ00327 10,0[a]	0.460 (9)	n.d.	n.d.	0.022 (38)	0.988 (19)	0.160 (6)	0.800 (16)	0.412 (9)	0.347 (8)
3CZ00327 20[a]	1.643 (29)[c]	0.0042 (10)	0.0041 (14)	0.048 (16)	0.982 (10)	0.156 (3)	0.792 (8)	n.d.	0.329 (4)
3CZ00327 22[a]	1.249 (40)[c]	0.0034 (10)	0.0043 (13)	0.058 (15)	0.996 (10)	0.157 (3)	0.798 (9)	0.392 (5)	0.333 (5)
3CZ00327 21[a]	3.060 (134)[c]	0.0027 (7)	0.0047 (11)	0.077 (12)	0.997 (8)	0.151 (2)	0.789 (7)	0.394 (4)	0.327 (4)
3CZ00327 23[a]	0.166 (7)	0.0100 (82)	0.0022 (108)	0.230 (150)	0.999 (53)	0.150 (13)	0.755 (41)	0.389 (22)	0.335 (20)
3CZ00327 24	0.374 (12)	0.0028 (58)	n.d.	n.d.	0.948 (47)	0.157 (11)	0.793 (33)	0.405 (19)	0.343 (16)
3CZ00327 25	0.201 (9)	0.0079 (59)	n.d.	0.500 (377)	1.005 (44)	0.181 (11)	0.809 (30)	0.399 (17)	0.338 (14)
3CZ00327 26	0.359 (15)	0.0053 (45)	n.d.	0.356 (283)	0.997 (37)	0.174 (9)	0.805 (26)	0.400 (15)	0.328 (13)
3CZ00327 27	0.287 (11)	0.0133 (58)	0.0089 (80)	0.156 (376)	0.991 (47)	0.176 (11)	0.832 (33)	0.422 (19)	0.347 (16)
3CZ00327 28	0.417 (23)	0.0048 (35)	0.0022 (47)	n.d.	0.969 (30)	0.165 (8)	0.793 (21)	0.417 (13)	0.337 (11)
3CZ00327 29	0.552 (26)	0.0055 (35)	0.0099 (51)	0.012 (217)	0.978 (32)	0.160 (8)	0.785 (23)	0.405 (13)	0.332 (12)
Mean	0.299 (44)								

Numbers in parentheses represent 1 standard deviation uncertainties in the unit of the last decimal place quoted.

[a] Preliminary ^{132}Xe concentrations and isotope ratios for *1 + 30* laser shot analyses for these samples were published in our previous paper (Crowther and Gilmour, 2012). The data here are for the summed analysis of 150 laser shots, performed as 1 single shot analysis followed by 5 analyses of 30 laser shots.

[b] The gas analysed in the initial, single laser shot extraction had an atmospheric isotopic composition, therefore this analyses has been excluded and the data here are the sum of the 5 analyses of 30 laser shots.

[c] Excluded from mean ^{132}Xe concentration calculations as a high concentration outlier.

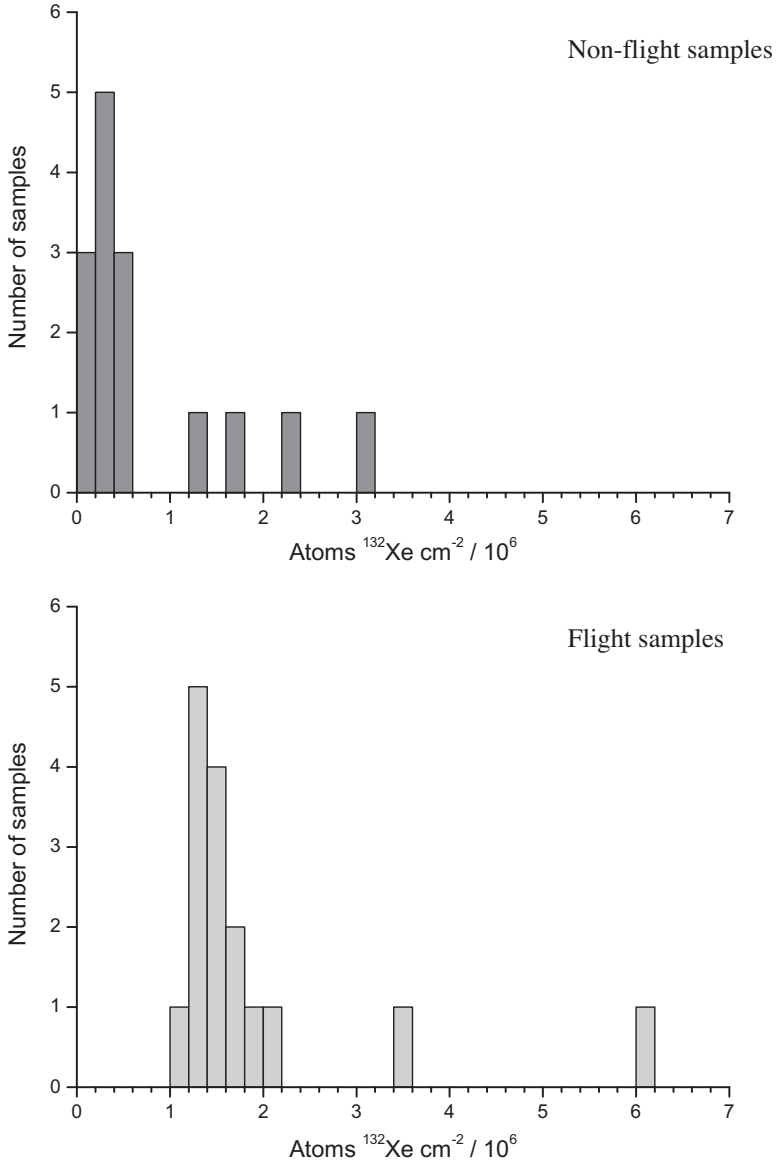

Fig. 1. Distribution of ^{132}Xe concentrations measured in non-flight (top) and flight (bottom) samples (Table 3). Non-flight samples contain blank xenon intrinsic to the collector targets; flight samples contain a mixture of blank xenon and implanted solar wind xenon. The ^{132}Xe concentrations in the majority of samples (both flight and non-flight) cluster together, with a small number of high concentration outliers. Mean ^{132}Xe concentrations (excluding the outliers) for both the flight and non-flight samples are given in Table 3. The ^{132}Xe concentration of the implanted solar wind is calculated from the difference between the mean ^{132}Xe concentration in the flight samples and that in the non-flight samples.

necessary to calculate the concentration of the implanted solar wind, i.e. make a correction to the flight samples for the intrinsic blank.

5.1. Blank correction

In our previous publication we investigated the possibility of using the intrinsic xenon at depth in samples to make a blank correction to the xenon in the implantation depth interval (Crowther and Gilmour, 2012). The data for those non-flight samples exhibited a linear correlation between the ^{132}Xe concentration in the implantation depth interval and that at depth. However there was no evidence of a similar correlation modified only by the implantation of solar wind into the upper depth interval for the flight samples.

We have investigated this further as more data became available. Fig. 3 shows the ^{132}Xe concentrations measured in the solar wind implantation depth interval by the first 150 laser shots (sum of 3 analyses) plotted as a function of the ^{132}Xe concentrations measured deeper in the samples (final 150 laser shot extraction). No correlation is observed for either the non-flight or the flight samples. Similar to Fig. 1, Fig. 3 shows that the majority of both the non-flight and flight samples cluster closely together, with a small

number of high ^{132}Xe concentration outliers. Therefore we conclude that it is not possible to use the concentrations of ^{132}Xe measured at depth in the samples, below the interval in which solar wind xenon is implanted, to make a blank correction to the ^{132}Xe concentrations measured in the implantation interval of the flight samples. However, the samples that we reject as outliers are enriched in "blank" xenon both in the solar wind implantation region and at depth.

Figs. 1 and 3 both illustrate that in both the flight and non-flight samples the ^{132}Xe concentrations measured in the majority of samples (in the implantation region and at depth) cluster tightly together with a narrow distribution that has a spread consistent with the uncertainties arising from sensitivity fluctuations in the instrument as measured by calibrations. In both cases a small number of high ^{132}Xe concentration outliers are observed, and exhibit unusually high concentrations both at depth and in the implantation region. These are best explained by addition of unusually large amounts of atmospheric blank (Fig. 2) from the samples in these extractions. Excluding these high concentration outliers, the mean measured ^{132}Xe concentration in the flight samples is $1.501(75) \times 10^6$ atoms ^{132}Xe cm^{-2}, and that in the non-flight samples is $0.299(44) \times 10^6$ atoms ^{132}Xe cm^{-2} (Table 3).

5.2. Solar wind xenon concentration and composition

The ^{132}Xe concentration of the implanted solar wind is determined from the difference between the mean ^{132}Xe concentrations for the flight and non-flight samples (after the outliers have been rejected, as discussed above). This gives the concentration of the implanted solar wind as $1.202(87) \times 10^6$ atoms ^{132}Xe cm^{-2}. The corresponding flux of ^{132}Xe ions is $(5.14 \pm 0.21) \times 10^6$ atoms cm^{-2} year^{-1} at the L1 point. This concentration is intermediate between, and in excellent agreement with, the concentrations of $1.25(9) \times 10^6$ atoms ^{132}Xe cm^{-2} determined by Vogel et al. (2011) and $1.15(4) \times 10^6$ atoms ^{132}Xe calculated from Meshik et al.'s (2012) analyses. The mean of these 3 separate analyses gives a concentration of 1.201×10^6 atoms ^{132}Xe cm^{-2}, with a standard deviation of 0.050×10^6. These values, however, are somewhat higher than the pre-mission predictions (Burnett et al., 2003) ($\sim 8 \times 10^5$ atoms ^{132}Xe cm^{-2}), even allowing for the fact that the pre-flight predictions were for the 2-year flux but the bulk collector arrays were actually continually exposed to the solar wind for 852.83 days (Reisenfeld et al., 2007).

Our calculated solar wind concentration is used in conjunction with the observed linear correlations between the measured isotope ratios and the reciprocal of the measured ^{132}Xe concentration (Fig. 2) to determine the isotopic composition of the implanted solar wind. This is similar to the technique used in the analysis of noble gases in lunar samples returned by the Apollo 11 mission (Eberhardt et al., 1970). In Fig. 2 we plot the measured isotope ratios against the reciprocal of the measured ^{132}Xe concentration. Eberhardt et al. (1970) assumed the measured ratios to be a mixture of components (trapped and spallation), each of fixed isotopic composition. Assuming the concentration (by mass) of the spallation component to be constant across a range of grain size fractions, they determined the isotopic composition of the trapped component from the intercept on the y-axis (1/concentration = 0) where the added trapped component would dominate the bulk composition. Here we assume the measured ratios to be a mixture of a variable amount of atmospheric xenon and a constant concentration (by surface area) of implanted solar wind xenon, and use the calculated concentration of the implanted solar wind ($1.202(87) \times 10^6$ atoms ^{132}Xe cm^{-2}) to determine its isotopic composition from the best fit lines (i.e. when the concentration of blank xenon is zero, so the measured concentration is equal to the concentration of the implanted solar wind). This isotopic composition is given in Table 4 and plotted as delta values relative to the terrestrial atmospheric composition in Fig. 4. In Fig. 5 the calculated composition for the major isotopes is also plotted as delta values relative to the solar wind xenon isotope ratios measured in the YLR (Pepin et al., 1995), where the scale allows any differences to be seen more clearly. Samples analysed in this work typically contained $\leqslant$700 atoms of ^{124}Xe or ^{126}Xe, hence the ratios for these isotopes are not as precise as for the more abundant isotopes. During these analyses isobaric hydrocarbons interfered with the ^{126}Xe and ^{128}Xe peaks in the mass spectrum, contributing additional uncertainty to these ratios (see Section 4 and Table 1 regarding corrections for procedural blank).

Our calculated Genesis solar wind isotope ratios are all within error of those determined from the young lunar regolith samples (Pepin et al., 1995) (Table 4 and Fig. 5), indicating excellent agreement of our data and the lunar data. The Genesis solar wind ratios determined by Meshik et al. (2012) are also within error of the ratios determined from the young lunar regolith (Table 4 and Fig. 5), although there are some minor discrepancies between our values and those of Meshik et al. The precision of Meshik et al.'s analyses is somewhat better than that of our analyses, primarily due to the size of samples used – typically 9–25 mm^2 in this work compared to samples of several cm^2 analysed by Meshik et al. This is most apparent for the ^{124}Xe/^{132}Xe and ^{126}Xe/^{132}Xe ratios: as noted above, samples analysed in this work typically contained $\leqslant$700 atoms of ^{124}Xe or ^{126}Xe. The ^{129}Xe/^{132}Xe ratio measured by Vogel et al. (2011) is higher than those determined in this work, by Meshik et al. (2012) and from the lunar samples.

Our calculated Genesis solar wind isotopic composition depends on the calculated ^{132}Xe concentration of the implanted solar wind. A different concentration would lead to different isotope ratios with correlated variations from our quoted composition. However, even if the isotopic composition is re-calculated for the upper and lower limits of the solar wind concentration we have determined, the new ratios all agree within uncertainty with the values given in Table 4. If we were to include the lowest concentration rejected outlier of the non-flight samples (as discussed above), the distributions of both the flight and non-flight samples would have similar standard deviations ($\sim$0.3). The solar wind concentration calculated in this way is within the range of our value, and the isotopic composition remains within the quoted error margins. The isotopic composition also depends on the lines of best fit used in

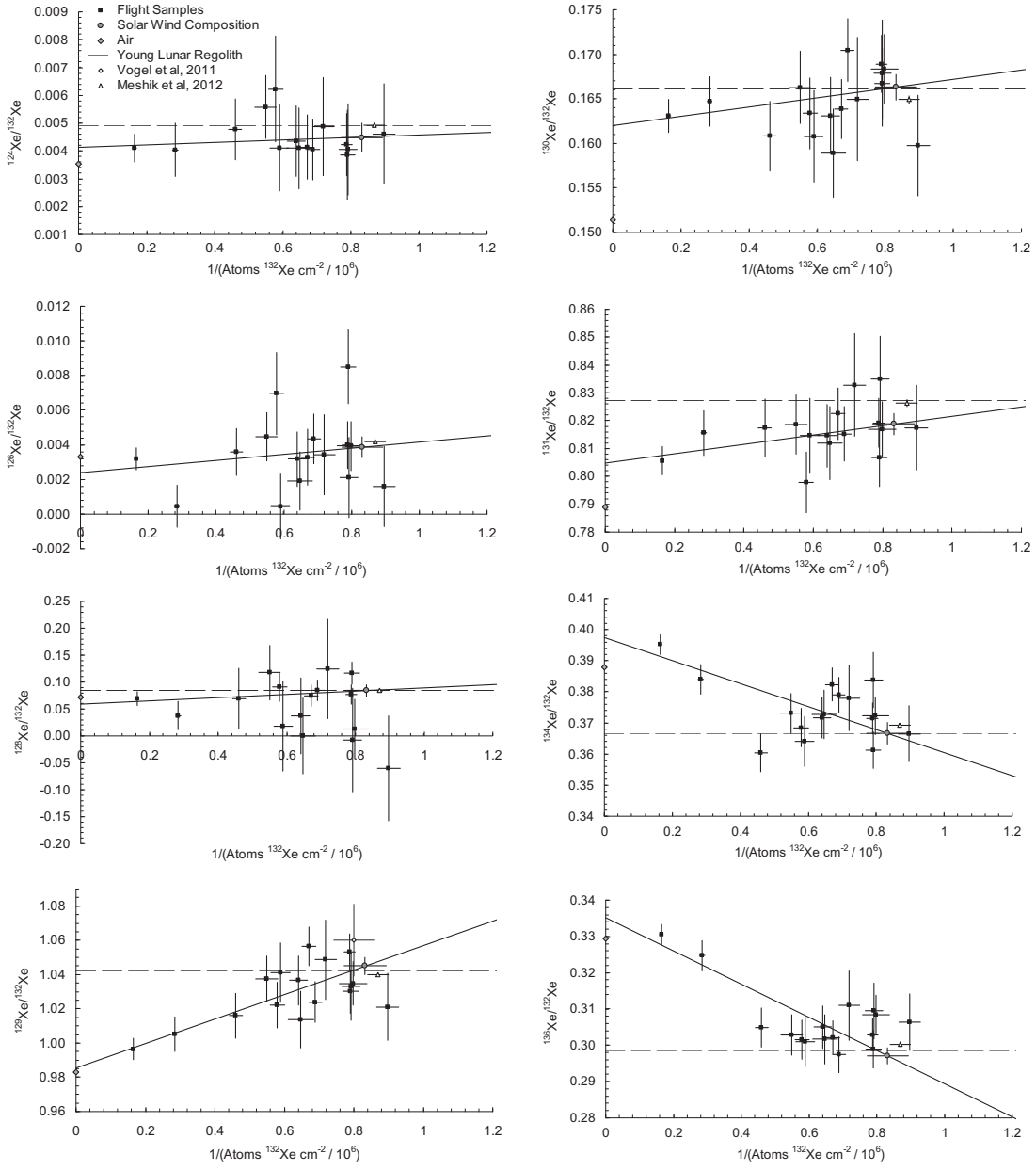

Fig. 2. Measured xenon isotopic ratios plotted as a function of the measured ^{132}Xe concentration (Table 3). The measured ratios trend towards atmospheric ratios as the measured ^{132}Xe concentration increased, as would be expected for a uniform concentration implanted solar wind component mixing with a variable concentration (atmospheric) blank component. The solid lines represent the best fit through the experimental data. These lines are used with the calculated solar wind concentration ($1.202(87) \times 10^6$ atoms ^{132}Xe cm^{-2}) to determine the isotopic composition of the implanted solar wind, which is plotted as dark grey circles and given in Table 4. Genesis ^{132}Xe concentrations and xenon isotope ratios measured by Meshik et al. (2012) and Vogel et al. (2011), and the solar wind xenon isotope ratios measured in the young lunar regolith (Pepin et al., 1995) are also plotted for reference.

Fig. 2. If the lines are forced to pass through the air end-member, the solar wind isotopic composition is again unchanged but the precision is artificially improved since an additional prior constraint has been introduced; our data demonstrate that the blank composition is consistent with that of the terrestrial atmosphere, but we have no grounds to assume it is exactly equal to that of the terrestrial atmosphere. We note that the ^{130}Xe/^{132}Xe ratio derived from this approach would be ~22‰ higher (less than 2 s.d.) than the ratio given in Table 4.

6. RELATIONSHIPS BETWEEN SOLAR WIND XENON AND OTHER SOLAR SYSTEM SIGNATURES

The evidence thus suggests that the lunar measurements are accurate representations of the solar wind. The Earth's

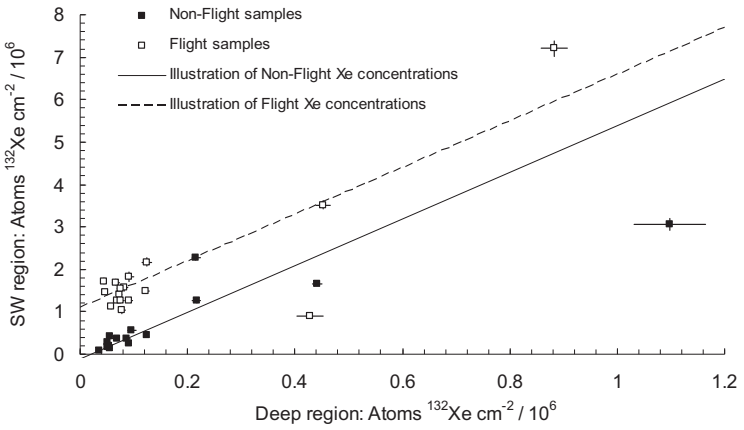

Fig. 3. ^{132}Xe concentrations measured in the "solar wind interval" (SW region, first 150 laser shots) plotted as a function of the final "deep xenon" (final 150 laser shots) extraction. Here the initial laser shot is included for sample 60927, as it is the measured concentrations, rather than ratios, which are of interest. It is not possible to fit a meaningful correlation line through the data points for either the flight or non-flight samples. The lines shown in this figure are purely to illustrate how we might expect the xenon concentrations measured in the flight to differ from those measured in the non-flight samples if a correlation between the xenon concentrations measured in solar wind interval and those measured at depth did exist. Samples that are enriched in blank xenon in the solar wind interval also appear to be enriched in blank xenon at depth.

atmosphere appears to be depleted in the heavy isotopes of xenon relative to a mass fractionated solar component. As noted above, the observed ratios cannot be obtained from *addition* of spontaneous fission products from ^{244}Pu and ^{238}U to mass fractionated solar wind. Hence the question of how the xenon composition observed in the Earth's atmosphere derived from the solar wind remains as yet unanswered. There is no evidence that solar wind xenon is depleted in the heavy isotopes relative to the composition measured in the young lunar regolith, i.e. SW-Xe is not similar to U-Xe, a component that has been proposed as the starting composition for the evolution of the Earth's atmosphere (Pepin, 2000).

Solar xenon reflects the integrated contributions from all nucleosynthetic sources that contributed to the solar system over the history of the galaxy. Lavielle and Marti (1992) showed that xenon trapped in ordinary chondrite meteorites is consistent with varying mixtures of Xe-HL and mass fractionated solar xenon. Gilmour (2010) examined the relationship between solar xenon (using the YLR composition) and two subtly different isotopic signatures present in meteorites: Xe-Q (Busemann et al., 2000) and Xe-P3 (Huss and Lewis, 1994). It was concluded that Xe-Q could be understood as mass fractionated solar xenon with minor contributions from exotic Xe-HL (Huss and Lewis, 1994) and monoisotopic ^{129}Xe from decay of ^{129}I. It seems likely that these are additions that vary from parent body to parent body to an underlying component trapped directly from the solar wind. In contrast, Xe-P3 could not be produced by addition of exotic or radiogenic components to mass fractionated solar xenon. Xe-P3 appeared to be xenon trapped by a process similar to the one that incorporated Xe-Q, but from a gas representative of an earlier period of galactic chemical evolution when the s-process had made a smaller contribution.

We now examine whether these relationships hold up when evaluated against the more precise composition of solar xenon derived from Genesis data. Details of the methodology can be found in Gilmour (2010); briefly, we determine a calculated composition of a target component by varying the contributions of known components and the degree of linear mass fractionation. The delta value of an isotopic ratio of the calculated composition (R_a) relative to the target composition (R_b) is defined as:

$$\delta(a,b) = 1000\left(\frac{R_a}{R_b} - 1\right) \tag{2}$$

The delta value for each isotope is divided by its associated uncertainty, which includes contributions from both components, and a χ^2 statistic is defined to evaluate the goodness of fit of the end composition to the target, and optimized. We define χ^2 as:

$$\chi^2 = \sum_i \left(\frac{\delta^i(a,b)}{\Delta^i}\right)^2 \tag{3}$$

where δ^i is the delta value for isotope i, as given by Eq. (2), and Δ^i is its uncertainty, derived from the uncertainties on both underlying ratios. Because contributions from ^{129}I decay are a possibly confounding factor, ^{129}Xe is excluded from the calculation of χ^2, there are thus 7 isotope ratios to consider. The number of degrees of freedom is given by difference between the number of isotope ratios under consideration and the number of parameters being varied. As different models can have difference number of parameters, we consider χ^2 per degree of freedom when comparing the quality of fit of different models. In the models discussed here we will use the Genesis solar wind data of Meshik et al. (2012) as they are generally more precise than either our or the lunar regolith data. The compositions of standard Xe components used in these models are in Table 5a; the compositions calculated from the model are in Table 5b and c. Table 6 summarises the percentage contributions of the different components and the degree of mass fractionation for each model, along with the χ^2 per degree of freedom.

We first consider Xe-Q (Table 5 and Fig. 6). The best fit involves mass fractionation of solar xenon by 8.1‰ amu^{-1}

Table 4
^{132}Xe concentration and isotope ratios of the present day solar wind xenon sampled by the Genesis mission. The solid lines in Fig. 2 represent the best fit through the measured isotope ratios and ^{132}Xe concentrations. The calculated solar wind ^{132}Xe concentration (1.202(87) × 10^6 atoms ^{132}Xe cm^{-2}) is used to determine the isotopic composition of the implanted solar wind from these lines of best fit. This isotopic composition is plotted as dark grey circles in Fig. 2.

	Atoms ^{132}Xe per cm^2 (×10^6)	^{124}Xe/^{132}Xe	^{126}Xe/^{132}Xe	^{128}Xe/^{132}Xe	^{129}Xe/^{132}Xe	^{130}Xe/^{132}Xe	^{131}Xe/^{132}Xe	^{134}Xe/^{132}Xe	^{136}Xe/^{132}Xe
This work	1.202 (87)	0.00449 (50)	0.00387 (60)	0.0840 (105)	1.0450 (50)	0.1663 (15)	0.8188 (39)	0.3667 (35)	0.2971 (23)
Meshik et al. (2012)	1.15 (4)	0.00492 (7)	0.00417 (9)	0.0842 (3)	1.0401 (10)	0.1649 (4)	0.8263 (13)	0.3692 (7)	0.3003 (6)
Vogel et al. (2011)	1.25 (9)				1.06 (1)				
Young Lunar Regolith		0.004897 (39)	0.00423 (14)	0.0848 (10)	1.042 (9)	0.16611 (91)	0.8272 (53)	0.3666 (25)	0.2985 (19)
Air			0.003537 (11)	0.003300 (17)	0.07136 (9)	0.9832 (12)	0.15136 (12)	0.7890 (11)	0.3879 (6)

Numbers in parentheses represent 1 standard deviation uncertainties in the unit of the last decimal place quoted.
Samples typically contained ⩽700 atoms of ^{124}Xe or ^{126}Xe, hence the isotope ratios for these isotopes are not as precise as the more abundant ones. Isobaric hydrocarbons interfere with the ^{126}Xe and ^{128}Xe peaks in the mass spectrum, contributing additional uncertainty to these ratios.
Genesis xenon isotope ratios measured by Meshik et al. (2012) and Vogel et al. (2011), the solar wind xenon isotope ratios measured in the young lunar regolith (Pepin et al., 1995) and the composition of terrestrial atmospheric xenon (Basford et al., 1973) are also given for reference.

favouring the heavy isotopes, and addition of Xe-HL (a 1.5% contribution to total ^{132}Xe), which yields χ^2 per degree of freedom of 1.6 (Table 6a). We contend that the simplest explanation of this is that the underlying composition of Xe-Q is mass fractionated solar xenon. On the assumption that the solar wind is not mass fractionated by the acceleration process, mass fractionation is associated with the trapping process. The contribution from Xe-HL appears to vary from ~0.2% to ~3.3% among the meteorites reported by Busemann et al. (2000), suggesting mixing of Xe-HL into an underlying composition that is mass fractionated solar xenon either during processing on the parent body or during the release process. The only isotope that varies from this pattern is ^{124}Xe; the ^{124}Xe/^{132}Xe ratio of Xe-Q is low by 23.6‰ (less than 2 s.d.) compared to the model. We return to this below.

Meshik et al. (2013) proposed that a small contribution of s-process Xe should be added to the mixture of fractionated solar wind Xe and Xe-HL. We find that this does not improve the fit; although adding a free parameter to the model inevitably reduces the best fit χ^2, the χ^2 per degree of freedom of the best fit model that includes s-process xenon is slightly larger than that without a s-process contribution (Table 6a). We conclude that there is no strong evidence of a contribution from s-process xenon to Xe-Q, and that the most parsimonious explanation does not include such a contribution. Gilmour (2010) noted that Kr-Q may include a contribution from s-process krypton, but noted that the model is under-constrained.

The proposed account of Xe-P3 also withstands the refinement in the composition of solar xenon (Table 5 and Fig. 7). The accepted composition is defined to lie on a mixing line through air and Xe-HL (Fig. 3, in Huss and Lewis, 1994), so the (1.1%) contribution from Xe-HL may or may not reflect a variation between its contribution to solar xenon and the Xe-P3 source. Xe-P3 cannot be produced from SW-Xe by the addition of other components; it requires the subtraction of an s-process contribution, a process which is not physically viable. In Fig. 7 and Table 5 SW-Xe has been mathematically modelled from a starting composition of Xe-P3 by linear mass fractionation and additions of Xe-HL and s-process Xe, as in Gilmour (2010). A simple model would involve Xe-P3 being trapped from a reservoir that subsequently evolved to SW-Xe by addition of s-process xenon (as noted, the apparent contribution of Xe-HL may arise from the definition of Xe-P3 on a mixing line to this component). The trapping process is presumed to be the source of the fractionation required in the model. Once again, neglecting the possibility of mass fractionation during the process that accelerates the solar wind, Xe-P3 appears to have been derived from an ambient gas by a trapping process that introduced the same mass fractionation as that which was responsible for trapping Xe-Q. However, the ambient gas had an s-process deficit (0.9% of ^{132}Xe) compared to solar xenon.

Once again ^{124}Xe is anomalous – Xe-P3 appears to have less than the required amount by 30.0‰ (less than 2 s.d.). We note that ^{124}Xe in the new composition of Meshik et al. (2012) is notably different from that of the young lunar regolith (Pepin et al., 1995), but reported at approximately the

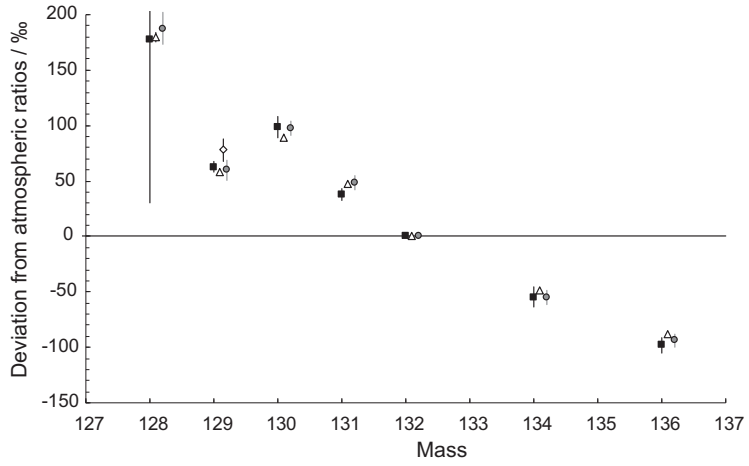

Fig. 4. Solar wind xenon composition (Table 4) plotted as delta values relative to atmospheric xenon. The minor isotopes have been excluded to allow the major isotopes to be illustrated more clearly. Samples typically contained ⩽700 atoms of ^{124}Xe or ^{126}Xe, hence the isotope ratios for these isotopes are not as precise as the more abundant ones. Isobaric hydrocarbons interfere with the ^{126}Xe and ^{128}Xe peaks in the mass spectrum, contributing additional uncertainty to these ratios. Genesis xenon isotope ratios measured by Meshik et al. (2012) and Vogel et al. (2011), and the solar wind xenon isotope ratios measured in the young lunar regolith (Pepin et al., 1995) are also plotted for reference. Points for a given isotope are slightly off-set from each other on the *x*-axis simply for clarity.

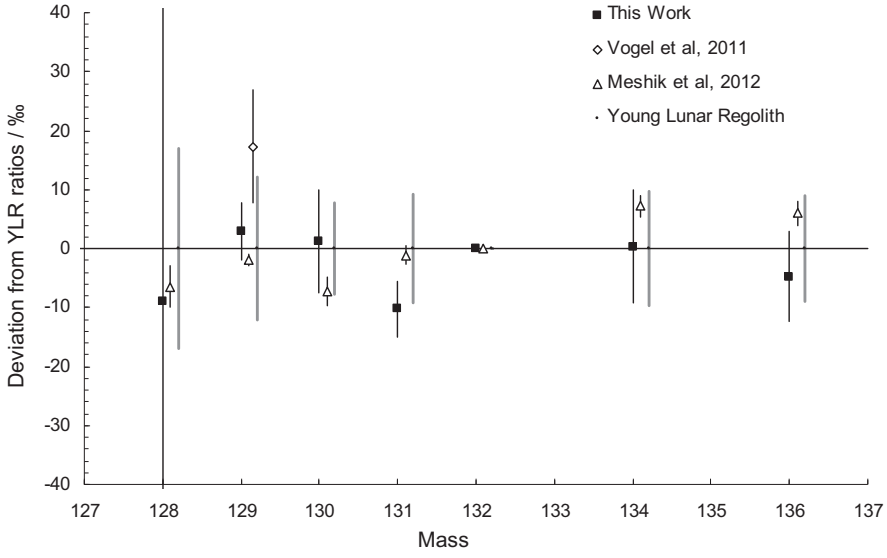

Fig. 5. Solar wind xenon composition (Table 4) plotted as delta values relative to the solar wind measured in the young lunar regolith (Pepin et al., 1995). Only the uncertainty in the Genesis isotope ratios has been taken into account when calculating the uncertainty of the delta values in this plot; the uncertainties of the solar wind xenon isotope ratios measured in the young lunar regolith (Pepin et al., 1995), are plotted separately as grey bars. The minor isotopes have been excluded to allow the major isotopes to be illustrated more clearly. An isobaric hydrocarbon interferes with the ^{128}Xe peak in the mass spectrum, contributing additional uncertainty to this ratio. Genesis xenon isotope ratios measured by Meshik et al. (2012) and Vogel et al. (2011) are also plotted for reference. Points for a given isotope are slightly off-set from each other on the *x*-axis simply for clarity.

same precision. In Fig. 6 and 7 we also present fits adopting a revised solar composition where the ^{124}Xe/^{132}Xe of Meshik et al. (2012) is replaced by a value based on the young lunar regolith measurement (Pepin et al., 1995). We note that while spallation effects in the lunar regolith could cause an overestimate of the ^{124}Xe/^{132}Xe ratio, this would not be monoisotopic and the variation observed requires the young lunar regolith ratio to be an *underestimate*. For this reason, and because of the relationship to other reservoirs in our solar system, we suggest the apparent high ^{124}Xe/^{132}Xe ratio reported by Meshik et al. (2012) is an artefact and that the revised composition (Table 5) is the best current estimate of the solar xenon composition. Further measurements will show whether this prediction based on our analysis is correct.

Using this revised composition, Xe-Q corresponds to a mixture of 98.4% SW-Xe, mass fractionated by 7.7‰ amu^{-1} favouring the heavy isotopes, mixed with 1.6% Xe-HL. As above, addition of a small contribution

Table 5
Compositions of xenon components and best fit models. (a) Lists the standard Xe components used in the models. (b) Contains the xenon solar wind composition determined by Meshik et al. (2012) and the model Xe-Q composition. It also contains a modelled composition of SW-Xe based on a starting composition of Xe-P3. (c) contains the corrected xenon solar wind composition (see text for details) along with the Xe-Q composition and modelled SW-Xe composition calculated from that corrected solar wind composition.

(a)

	Standard Xe components used in models			
	Xe-Q[a]	Xe-P3[b]	Xe-HL[b]	Xe-s[c]
$^{124}Xe/^{132}Xe$	0.00455 (2)	0.00446 (6)	0.00833 (9)	0.00000 (65)
$^{126}Xe/^{132}Xe$	0.004057 (18)	0.00400 (4)	0.00564 (8)	0.0000 (2)
$^{128}Xe/^{132}Xe$	0.0822 (2)	0.0806 (2)	0.0905 (6)	0.212 (4)
$^{129}Xe/^{132}Xe$	1.042 (2)	1.042 (4)	1.056 (2)	0.105 (30)
$^{130}Xe/^{132}Xe$	0.1619 (3)	0.1589 (2)	0.1542 (3)	0.48 (1)
$^{131}Xe/^{132}Xe$	0.8185 (9)	0.8247 (10)	0.8457 (13)	0.184 (18)
$^{134}Xe/^{132}Xe$	0.378 (11)	0.3767 (10)	0.6356 (13)	0.013 (5)
$^{136}Xe/^{132}Xe$	0.3164 (8)	≡0.3096	≡0.6991	≡0.0

(b)

	SW-Xe[d]	Xe-Q model	SW-Xe model[f]
$^{124}Xe/^{132}Xe$	0.00492 (7)	0.00466 (6)	0.00477 (6)
$^{126}Xe/^{132}Xe$	0.00417 (9)	0.00399 (8)	0.00419 (4)
$^{128}Xe/^{132}Xe$	0.0842 (3)	0.0816 (3)	0.0847 (2)
$^{129}Xe/^{132}Xe$	1.0401 (10)	1.0154 (10)	1.0604 (5)
$^{130}Xe/^{132}Xe$	0.1649 (4)	0.1621 (4)	0.1646 (2)
$^{131}Xe/^{132}Xe$	0.8263 (13)	0.8200 (13)	0.8261 (10)
$^{134}Xe/^{132}Xe$	0.3692 (7)	0.3791 (7)	0.3697 (10)
$^{136}Xe/^{132}Xe$	0.3003 (6)	0.3159 (6)	0.3002 (0)

(c)

	Revised SW-Xe[e]	Rev. Xe-Q model	Rev. SW-Xe model[f]
$^{124}Xe/^{132}Xe$	0.00481 (6)	0.00458 (6)	0.00475 (6)
$^{126}Xe/^{132}Xe$	0.00417 (9)	0.00400 (8)	0.00418 (4)
$^{128}Xe/^{132}Xe$	0.0842 (3)	0.0817 (3)	0.0846 (2)
$^{129}Xe/^{132}Xe$	1.0401 (10)	1.0167 (10)	1.0590 (5)
$^{130}Xe/^{132}Xe$	0.1649 (4)	0.1622 (4)	0.1645 (2)
$^{131}Xe/^{132}Xe$	0.8263 (13)	0.8204 (13)	0.8256 (10)
$^{134}Xe/^{132}Xe$	0.3692 (7)	0.3792 (7)	0.3696 (10)
$^{136}Xe/^{132}Xe$	0.3003 (6)	0.3159 (6)	0.3002 (0)

[a] Xe-Q data from Busemann et al. (2000).
[b] Xe-P3 and Xe-HL data from Huss and Lewis (1994), renormalized by Busemann et al. (2000).
[c] s-Process Xe data from Gilmour and Turner (2007).
[d] SW-Xe data from Meshik et al. (2012).
[e] Revised SW-Xe in which the $^{124}Xe/^{132}Xe$ of Meshik et al. (2012) is replaced by a value based on the young lunar regolith measurement (Pepin et al., 1995).
[f] Modelled SW-Xe composition based on a starting composition of Xe-P3. Xe-P3 was trapped from an ambient gas by a processes that introduced the same mass fractionation as that which trapped Xe-Q. However the ambient gas had an s-process deficit relative to SW-Xe.

of s-process Xe does not improve the quality of the fit (Table 6a). The ambient gas from which Xe-P3 was trapped had a 1.0% deficit of s-process Xe compared to SW-Xe. Trapping of Xe-P3 from this reservoir introduced a mass fractionation of 8.3‰ amu^{-1} favouring the heavy isotopes. These naturally show much better agreement of the ^{124}Xe ratios than previously. The χ^2 per degree of freedom is also smaller in both cases than for the models using Meshik et al.'s (2012) $^{124}Xe/^{132}Xe$ ratio (Table 6), indicating a better quality of fit for the models using the revised $^{124}Xe/^{132}Xe$ SW-Xe ratio.

6.1. An s-process deficit in xenon

The identification of a meteoritic xenon component deficient in s-process isotopes provides an interesting resonance with reports of s-process deficits in molybdenum (e.g. Dauphas et al., 2004; Burkhardt et al., 2012). Nicolussi et al. (1998) identified the isotopic composition of pure s-process molybdenum in silicon carbide grains from Murchison. ^{96}Mo is only produced by the s-process; it is shielded from the r-process. Relative to terrestrial standards, s-process molybdenum is strongly depleted in ^{92}Mo and ^{94}Mo (both produced by the p-process) and ^{100}Mo (produced by the r-process). Burkhardt et al. (2012) measured values of up to ~30 for $\varepsilon^{92}Mo$ in acid leachates of Murchison. A positive value for $\varepsilon^{92}Mo$ indicates a deficiency in ^{96}Mo, i.e. a deficiency in pure s-process molybdenum, relative to terrestrial standards. A ~0.3% contribution of s-process ^{96}Mo is needed to obtain the terrestrial $^{92}Mo/^{96}Mo$ ratio from this measured ratio. This is comparable to the ~2.8% contribution from the s-process only isotope ^{130}Xe in our models of

Table 6
Summary of contributions of standard components and degrees of mass fractionation for the models of Xe-Q and Xe-P3. Percentages are given for ^{132}Xe. The χ^2 per degree of freedom, indicating the relative quality of the fit, is also given for each model.

(a) Models of Xe-Q

SW-Xe (%)	Fractionation (‰ amu^{-1})	Xe-HL (%)	s-Process Xe (%)	χ^2 per degree of reedom	Source
98.5	10.2	1.5		0.3	Gilmour[a]
98.5	8.1	1.5		1.6	This work, using Meshik et al.'s SW-Xe[b]
98.3	8.4	1.6	0.1	1.7	This work, using Meshik et al.'s SW-Xe[b]
98.4	7.7	1.6		1.0	This work, using corrected SW-Xe[c]
98.2	7.9	1.7	0.1	1.1	This work, using corrected SW-Xe[c]

(b) Models of SW-Xe from Xe-P3

Xe-P3 (%)	Xe-HL (%)	Fractionation (‰ amu^{-1})	s-process Xe (%)	χ^2 per degree of freedom	Source
98.5	1.5	11.2	1.1	0.4	Gilmour[a]
98.9	1.1	8.7	0.9	1.3	This work, using Meshik et al.'s SW-Xe[b]
99.0	1.0	8.3	0.9	0.7	This work, using corrected SW-Xe[c]

[a] Models from Gilmour (2010).
[b] Models using the Genesis Solar Wind Xe ratios from Meshik et al. (2012).
[c] Model uses the revised SW-Xe composition – see text and Table 5 for details.

solar wind xenon. But whether the carriers responsible for the s-process deficit in Xe also have an s-process deficit in Mo (and vice versa) is unknown; we are not aware of molybdenum analyses of nanodiamond residues.

It seems that one or more presolar phases were present in the early solar system that recorded the isotopic composition of the galaxy earlier in its history, when the s-process had made a smaller contribution to the isotopic inventory. A further insight can be gained from the presence of a ^{129}Xe anomaly in Xe-P3 relative to the mass fractionated composition. Gilmour et al. (2005) demonstrated that the ^{129}Xe/^{132}Xe ratio of the Xe-P3 component in nanodiamonds varied systematically with the petrologic type of the parent meteorite, showing that the associated ^{129}I was alive in the early solar system. If this was incorporated at the same time as Xe-P3 was trapped, the trapping process could have occurred no more than $\sim 10^8$ years before solar system formation. An "initial" iodine ratio for this component (i.e. the ratio that pertained on last closure to xenon loss) could provide further information.

6.2. Model for the evolution of P3 and Q Xenon components

The P3 and Q xenon components exhibit a remarkable similarity apart from the s-process deficit apparent in Xe-P3. Although they have slightly different isotopic compositions, both appear mass fractionated to the same extent from a putative ambient gas component – the ambient gas component corresponding to Xe-P3 could have evolved into the component corresponding to Xe-Q (solar xenon) by addition of s-process xenon. Unless this reflects an unexpected mass fractionation of solar wind xenon with respect

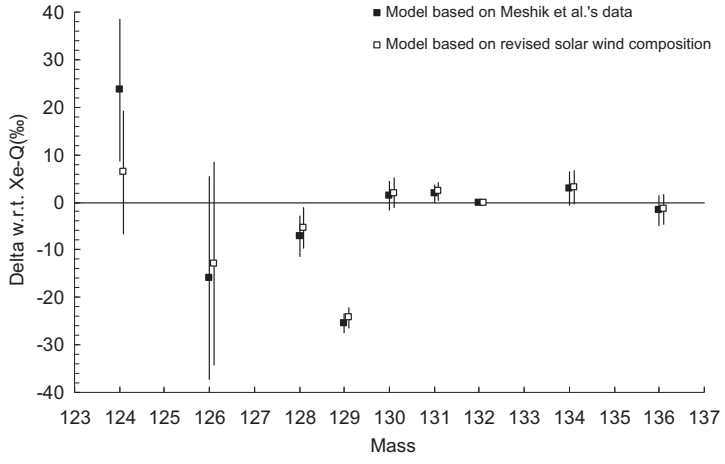

Fig. 6. Models of Xe-Q derived from mixtures of SW-Xe and Xe-HL. The model based on the SW-Xe composition determined by Meshik et al. (2012) corresponds to a mixture of 98.5% SW-Xe, mass fractionated by 8.1‰ amu^{-1} favouring the heavy isotopes mixed with 1.5% Xe-HL. The model based on the revised SW-Xe composition uses a ^{124}Xe/^{132}Xe ratio based on the lunar data (Pepin et al., 1995), and corresponds to a mixture of 98.4% SW-Xe, mass fractionated by 7.7‰ amu^{-1} favouring the heavy isotopes mixed with 1.6% Xe-HL.

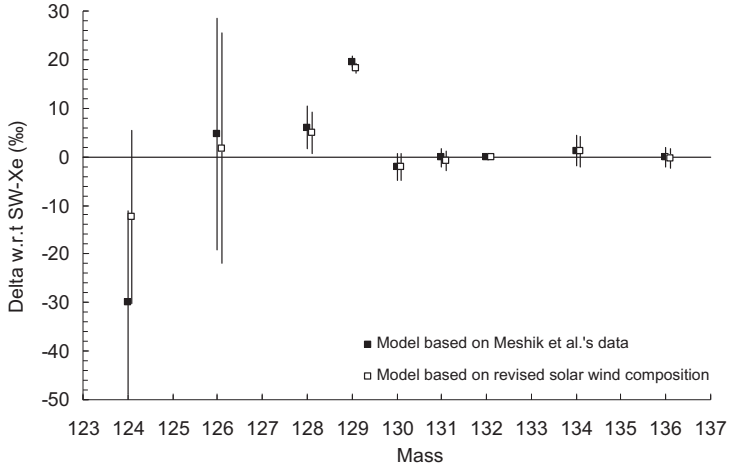

Fig. 7. Modelled composition of SW-Xe based on a starting composition of Xe-P3. In these models SW-Xe has been mathematically modelled by linear mass fractionation of Xe-P3 and additions of Xe-HL and s-process Xe. The contributions of each component and the degree of mass fractionation are summarised in Table 6b. Xe-P3 was trapped from an ambient gas by a process that introduced the same mass fractionation as that which trapped Xe-Q. However the ambient gas was deficient in s-process Xe relative to SW-Xe.

to the bulk xenon composition of the solar system, it is indicative of a similar trapping process having occurred in different environments separated in time and space on an astronomical scale. In addition, both exhibit excesses of ^{129}Xe relative to their parent, ambient gas, requiring high I/Xe ratios in their host phase ($\sim 10^3$ times higher than in the ambient gas). This high ratio must have held during solar system formation; the excess of ^{129}Xe associated with Xe-P3 varies differently from the other isotopes with

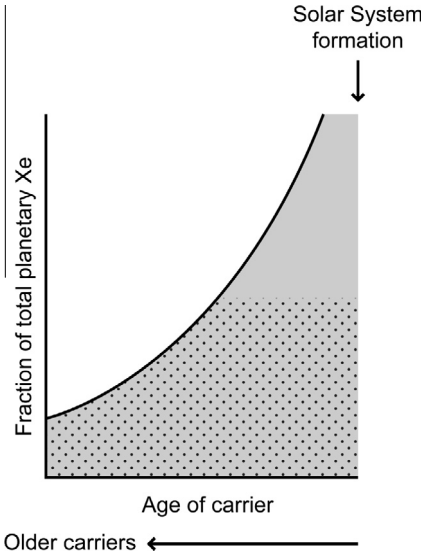

Fig. 8. Tentative qualitative model for the evolution of xenon components. The area shaded grey represents organic matter in bulk meteorites, which contain the integrated trapped xenon composition of all surviving carriers – Xe-Q. Younger, less robust carriers do not survive the acid treatments necessary to produce nanodiamond residues; only the more robust carriers survive – highlighted as the dotted area. Xe-P3 contains a larger proportion of carriers that sampled an earlier stage of galactic evolution when the contribution from the s-process was smaller.

petrologic type, indicating that it was present as ^{129}I during parent body processing. Such elemental fractionation is strongly indicative of a process involving "chemistry", such as adsorption, rather than implantation.

Xe-P3 is consistent with trapping from a single reservoir that subsequently evolved to solar xenon by addition of s-process material; this might be seen as a one end-member model. An alternative model (Fig. 8) is of environments where xenon (and iodine) are incorporated into organic carriers with fractionation of xenon isotopes occurring quasi-continuously in the history of material that contributed to our solar system. Some of the carriers are more resistant to destruction than others, so that longer lived carriers integrate the evolving xenon isotopic composition over a longer period than shorter-lived carriers. Less robust carriers are destroyed over shorter timescales; in bulk meteorites the carrier population is dominated by the more recent, less robust carriers that incorporated xenon after the last input of freshly synthesised material. The integrated composition of all surviving carriers (the area shaded grey in Fig. 8) dominated by material with recently trapped xenon is what we call Xe-Q. The acid treatment that produces nanodiamond-rich residues preferentially removes some of the less robust carriers, allowing the contribution from the longer-lived, more robust, carriers (the dotted area in Fig. 8) to become apparent. Thus Xe-P3 has a higher contribution of carriers that sampled an earlier stage of galactic chemical evolution when the contribution from s-process Xe was smaller.

The identical processes leading to incorporation imply that the mass fractionated solar xenon that underlies Xe-Q might be considered a presolar component (the incorporation of which occurred in a similar environment to the incorporation of isotopically distinct xenon reflected in the P3 component). However, our model does not involve the nature of the processes by which Xe was incorporated into organic carriers. Beyond suggesting that it has occurred more than once over the period of galactic

history sampled by surviving organic material in our solar system, and was possibly a widespread occurrence, we do not constrain the site or mechanism here. Both the interstellar medium (e.g. Huss and Alexander, 1987) and the early solar nebular (e.g. Ozima et al., 1998) have been proposed as sites where Phase Q gases may have been incorporated into organic carriers; in our model the latter requires recycling of material into the galaxy from other stellar nebulae. Various trapping mechanisms have also been proposed, including active capture and anomalous adsorption (Hohenberg et al., 2002) and adsorption of ions (Marrocchi et al., 2011), either of which may be consistent with the account of the origin of Xe-Q and Xe-P3 we propose. We propose that a key test of such models would be their efficacy in producing phases with high I/Xe ratios.

7. CONCLUSIONS

The fluence and composition of solar wind xenon trapped in silicon collectors from the Genesis mission has been determined. The fluence of implanted solar wind xenon is $1.202(87) \times 10^6$ atoms ^{132}Xe cm^{-2}, which equates to a flux of $(5.14 \pm 0.21) \times 10^6$ atoms ^{132}Xe cm^{-2} year^{-1}. This is in excellent agreement with the fluences reported by Vogel et al. (2011) and Meshik et al. (2012). The isotopic composition is consistent with that extracted from other Genesis collector targets and from the young lunar regolith. The question of how the xenon composition observed in the Earth's atmosphere originated remains.

The more precise composition of solar wind xenon confirms previously hypothesised relationships among solar wind xenon, Xe-Q, Xe-HL and Xe-P3. The underlying composition of Xe-Q is mass fractionated SW-Xe, with small, varying additions of ^{129}Xe from the decay of ^{129}I and Xe-HL. Xe-P3 is deficient in s-process xenon compared to SW-Xe. It is mass fractionated to the same extent as Xe-Q relative to a composition that can evolve to SW-Xe by addition of s-process material. This suggests the same trapping mechanism operating in similar environments at different times in galactic history. Xe-P3 may sample one presolar reservoir that subsequently evolved to solar xenon through addition of s-process material. Alternatively, it may be sourced from multiple trapping sites, with a more robust subset selected by preparation of a nanodiamond-rich residue having, on average, trapped xenon at an earlier stage of chemical evolution than Xe-Q.

ACKNOWLEDGEMENTS

We thank the Genesis mission team and the Genesis Solar Wind Sample Curation Team led by Don Burnett for their time and hard work in acquiring, selecting, characterising and cleaning samples. Thank you to R. Wieler, K. Marti, C. Hohenberg and Associate Editor G. Herzog for their helpful comments and reviews. This work was funded by the Science and Technology Facilities Council (STFC) Grant No. ST/J001643/1.

REFERENCES

Basford J. R., Dragon J. C., Pepin R. O., Coscio Jr. M. R. and Murthy V. R. (1973). Krypton and xenon in lunar fines. In *Proc. 4th Lunar Sci. Conf.*, vol. 2. pp. 1915–1955.

Benkert J. P., Baur H., Signer P. and Wieler R. (2012) He, Ne, and Ar from the solar-wind and solar energetic particles in lunar ilmenites and pyroxenes. *J. Geohpys. Res. [Planets]* **98**, 13147–13162.

Burkett P. J., Rodriguez M. C. and Allton J. H. (2011) Nuts and bolts – techniques for Genesis sample curation. *Lunar Planet. Sci. XLII*. Lunar Planet Inst., Houston. #1964 (abstr.).

Burkhardt C., Kleine T., Dauphas N. and Wieler R. (2012) Origin of isotopic heterogeneity in the solar nebula by thermal processing and mixing of nebular dust. *Earth Planet. Sci. Lett.* **357–358**, 298–307.

Burnett D. S., Barraclough B. L., Bennett R., Neugebauer M., Oldham L. P., Sasaki C. N., Sevilla D., Smith N., Stansbery E., Sweetnam D. and Wiens R. C. (2003) The Genesis discovery mission: return of solar matter to Earth. *Space Sci. Rev.* **105**, 509–534.

Burnett D. S. and Genesis Science Team (2011) Solar composition from the Genesis Discovery Mission. In *Proceedings of the National Academy of Sciences*, vol. 108. pp.19147–19151.

Busemann H., Baur H. and Wieler R. (2000) Primordial noble gases in "phase Q" in carbonaceous and ordinary chondrites studied by closed-system stepped etching. *Meteorit. Planet. Sci.* **35**, 949–973.

Calaway M. J., Burnett D. S., Rodriguez M. C., Sestak S., Allton J. H. and Stansbery E. K. (2007) Decontamination of Genesis Array Materials by UV Ozone Cleaning. *Lunar Planet. Sci. XXXVIII*. Lunar Planet Inst., Houston. #1627 (abstr.).

Calaway M. J., Rodriguez M. C., Allton J. H. and Stansbery E. K. (2009) Decontaminating solar wind samples with the Genesis ultra-pure water megasonic wafer spin cleaner. *Lunar Planet. Sci. XL*. Lunar Planet Inst., Houston. #1183 (abstr.).

Crowther S. A. and Gilmour J. D. (2012) Measuring the elemental abundance and isotopic signature of solar wind xenon collected by the Genesis Mission. *J. Anal. At. Spectrom.* **27**, 256–269.

Crowther S. A., Filtness M. J. and Gilmour J. D. (2008) Applications of RELAX to xenon measurements in genesis samples. *Lunar Planet. Sci. XXXIX*. Lunar Planet Inst., Houston. #1762 (abstr.).

Crowther S. A., Mohapatra R. K., Turner G., Blagburn D. J., Kehm K. and Gilmour J. D. (2008b) Characteristics and applications of RELAX, an ultrasensitive resonance ionization mass spectrometer for xenon. *J. Anal. At. Spectrom.* **23**, 938–947.

Dauphas N., Davis A. M., Marty B. and Reisberg L. (2004) The cosmic molybdenum-ruthenium isotope correlation. *Earth Planet. Sci. Lett.* **226**, 465–475.

Eberhardt P., Geiss J., Graf H., Grögler N., Krähenbühl U., Schwaller H., Schwarzmüller J. and Stettler A. (1970) Trapped solar wind noble gases, exposure age and K/Ar-age in Apollo 11 lunar fine material. In *Apollo 11 Lunar Science Conference*. Pergamon Press, Inc., Houston, TX. pp. 1037–1070.

Geiss J., Bühler F., Cerutti H., Eberhardt P., Filleux C., Meister J. and Signer P. (2004) The Apollo SWC experiment: results, conclusions, consequences. *Space Sci. Rev.* **110**, 307–335.

Gilmour J. D. (2010) "Planetary" noble gas components and the nucleosynthetic history of solar system material. *Geochim. Cosmochim. Acta* **74**, 380–393.

Gilmour J. D. and Turner G. (2007) Constraints on nucleosynthesis from xenon isotopes in presolar material. *Atsrophys. J.* **657**, 600–608.

Gilmour J. D., Hewett S. M., Lyon I. C., Stringer M. and Turner G. (1991) A resonance ionization mass-spectrometer for xenon. *Meas. Sci. Technol.* **2**, 589–595.

Gilmour J. D., Lyon I. C., Johnston W. A. and Turner G. (1994) Relax – an ultrasensitive, resonance ionization mass-spectrometer for xenon. *Rev. Sci. Instrum.* **65**, 617–625.

Gilmour J. D., Verchovsky A. B., Fisenko A. V., Holland G. and Turner G. (2005) Xenon isotopes in size separated nanodiamonds from Efremovka: $^{129}Xe^{*}$, Xe-P3, and Xe-P6. *Geochim. Cosmochim. Acta* **69**, 4133–4148.

Heber V. S., Wieler R., Baur H., Olinger C., Friedmann T. A. and Burnett D. S. (2009) Noble gas composition of the solar wind as collected by the Genesis mission. *Geochim. Cosmochim. Acta* **73**, 7414–7432.

Hohenberg C. M., Thonnard N. and Meshik A. (2002) Active capture and anomalous adsorption: new mechanisms for the incorporation of heave noble gases. *Meteorit. Planet. Sci.* **37**, 257–267.

Huss G. R. and Alexander E. C. (1987) On the presolar origin of the "normal planetary" noble gas component in meteorites. *Proc. 17th Lunar Planet. Sci. Conf.. J. Geophys. Res. Solid Earth* **92**, E710–E716.

Huss G. R. and Lewis R. S. (1994) Noble gases in presolar diamonds I: three distinct components and their implications for diamond origins. *Meteoritics* **29**, 791–810.

Jurewicz A. J. G., Burnett D. S., Wiens R. C., Friedmann T. A., Hays C. C., Hohlfelder R. J., Nishiizumi K., Stone J. A., Woolum D. S., Becker R., Butterworth A. L., Campbell A. J., Ebihara M., Franchi I. A., Heber V., Hohenberg C. M., Humayun M., McKeegan K. D., McNamara K., Meshik A., Pepin R. O., Schlutter D. and Wieler R. (2003) The Genesis solar-wind collector materials. *Space Sci. Rev.* **105**, 535–560.

Lavielle B. and Marti K. (1992) Trapped xenon in ordinary chondrites. *J. Geophys. Res.* **97**, 20875–20881.

Marrocchi Y., Marty B., Reinhardt P. and Robert F. (2011) Adsorption of xenon ions onto defects in organic surfaces: implications for the origin and the nature of organics in primitive meteorites. *Geochim. Cosmochim. Acta* **75**, 6255–6266.

Meshik A., Hohenberg C., Pravdivtseva O. and Burnett D. (2012) Measuring the isotopic composition of solar wind noble gases. In Exploring the Solar Wind. InTech. (ed. M. Lazar). pp. 93–120.

Meshik A., Hohenberg C. M., Pravdivtseva O. and Burnett D. S. (2013). Xenon isotopes in aluminum solar wind collectors from Genesis Mission. *Lunar Planet. Sci. XLIV*. Lunar Planet Inst., Houston. #3103 (abstr.).

Nicolussi G. K., Pellin M. J., Lewis R. S., Davis A. M., Amari S. and Clayton R. N. (1998) Molybdenum isotopic composition of individual presolar silicon carbide grains from the Murchison meteorite. *Geochim. Cosmochim. Acta* **62**, 1093–1104.

Ozima M., Wieler R., Marty B. and Podoske F. A. (1998) Comparative studies of solar, Q-gases and terrestrial noble gases, and implication of the evolution of the solar Nebula. *Geochim. Cosmochim. Acta* **62**, 301–314.

Palma R. L., Becker R. H., Pepin R. O. and Schlutter D. J. (2002) Irradiation records in regolith materials, II: solar wind and solar energetic particle components in helium, neon, and argon extracted from single lunar mineral grains and from the Kapoeta howardite by stepwise pulse heating. *Geochim. Cosmochim. Acta* **66**, 2929–2958.

Pepin R. O. (2000) On the isotopic composition of primordial xenon in terrestrial planet atmospheres. *Space Sci. Rev.* **92**, 371–395.

Pepin R. O., Becker R. H. and Rider P. E. (1995) Xenon and krypton isotope in extraterrestrial regolith soils and in the solar-wind. *Geochim. Cosmochim. Acta* **59**, 4997–5022.

Reisenfeld D. B., Burnett D. S., Becker R. H., Grimberg A. G., Heber V. S., Hohenberg C. M., Jurewicz A. J. G., Meshik A., Pepin R. O., Raines J. M., Schlutter D. J., Wieler R., Wiens R. C. and Zurbuchen T. H. (2007) Elemental abundances of the bulk solar wind: analyses from Genesis and ACE. *Space Sci. Rev.* **130**, 79–86.

Russell S. S. (2007) The formation of the solar system. *J. Geol. Soc.* **164**, 481–492.

Sestak S., Franchi I. A., Verchovsky A. B., Al-Kuzee J., Braithwaite N. S. J., Burnett D. S. and Stansbery E. (2006) Application of semiconductor industry cleaning technologies for Genesis sample collectors. *Lunar Planet. Sci. XXXVII*. Lunar Planet Inst., Houston. #1878 (abstr.).

Turcotte S. and Wimmer-Schweingruber R. F. (2002) Possible in situ tests of the evolution of elemental and isotopic abundances in the solar convection zone. *J. Geophys. Res.* **107**, 1442.

Vogel N., Heber V. S., Baur H., Burnett D. S. and Wieler R. (2011) Argon, krypton, and xenon in the bulk solar wind as collected by the Genesis mission. *Geochim. Cosmochim. Acta* **75**, 3057–3071.

Wieler R. and Baur H. (1994) Krypton and xenon from the solar wind and solar energetic particles in two lunar ilmenites of different antiquity. *Meteoritics* **29**, 570–580.

Wiens R. C., Bochsler P., Burnett D. S. and Wimmer-Schweingruber R. F. (2004) Solar and solar-wind isotopic compositions. *Earth Planet. Sci. Lett.* **222**, 697–712.

Associate editor: Gregory F. Herzog